

**Nanofluid flow over a flat surface induced by stream  
wise pressure gradient utilizing different  
mathematical models**



by

**Ammara Bhatti**

A thesis submitted in partial fulfilment of the requirements for the degree of  
Master of Science in Mathematics

Supervised by



**Dr. Meraj Mustafa Hashmi**

Department of Mathematics, School of Natural Sciences, National University of  
Sciences and Technology, Islamabad, Pakistan

©Ammara Bhatti, 2021

**National University of Sciences & Technology****MS THESIS WORK**

We hereby recommend that the dissertation prepared under our supervision by: Ammara Bhatti, Regn No. 00000321366 Titled: "Nanofluid flow over a flat surface induced by stream-wise pressure gradient utilizing different mathematical models" accepted in partial fulfillment of the requirements for the award of **MS** degree.

**Examination Committee Members**1. Name: DR. MUJEEB UR REHMANSignature: 2. Name: DR. MUHAMMAD ASIF FAROOQSignature: External Examiner: DR. NASIR ALISignature: Supervisor's Name: DR. MERAJ MUSTAFA HASHMISignature: 
  
 Head of Department

21/09/2021  
 Date
**COUNTERSIGNED**Date: 22.09.2021
  
 Dean/Principal

*This thesis is dedicated to my family for their constant support  
and to my friends for always encouraging me.*

## THESIS ACCEPTANCE CERTIFICATE

Certified that final copy of MS/MPhil thesis written by Mr/Ms **Ammara Bhatti**, (Registration No.**00000321366**), of School of Natural Sciences has been vetted by undersigned, found complete in all respects as per NUST Statutes/Regulations, is free of plagiarism, errors, and mistakes and is accepted as partial fulfilment for award of MS/MPhil degree. It is further certified that necessary amendments as pointed out by GEC members and external examiner of the scholar have also been incorporated in the said thesis.

Signature: \_\_\_\_\_

Name of Supervisor: \_\_\_\_\_

Date: \_\_\_\_\_

Signature (HoD): \_\_\_\_\_

Date: \_\_\_\_\_

Signature (Dean/Principal): \_\_\_\_\_

Date: \_\_\_\_\_

**National University of Sciences and Technology**

**MS THESIS WORK**

We here by recommend that the thesis prepared under our supervision by:  
Mr/Ms.....Titled:.....  
..... be accepted  
in partial fulfilled the requirements for the award of MS degree.

**Examination Committee Members**

- 1. Name.....Signature: .....
- 2. Name.....Signature: .....
- 3. Name.....Signature: .....
- 4. Name.....Signature: .....

Supervisor's Name.....Signature: .....

Head of Department's Signature.....Date.....

**COUNTERSIGNED**

Principal/Dean.....Date.....

# Table of Contents

<i>Acknowledgments</i> .....	v
Abstract .....	6
Chapter 1 .....	7
Introduction.....	7
1.1 Boundary Layer Flow .....	7
1.2 Falkner-Skan Flow .....	8
1.3 Nanofluids.....	9
1.4 Mathematical Models for Thermal Transport Using Nanofluids .....	10
1.4.1 Tiwari and Das Model .....	10
1.4.2 Buongiorno Model.....	11
1.5 Slip and No-slip Boundary Conditions .....	12
1.6 Some Dimensionless Numbers .....	12
1.6.1 Reynolds Number .....	12
1.6.2 Schmidt Number .....	12
1.6.2 Prandtl Number .....	12
1.6.3 Grashof Number.....	13
1.6.5 Nusselt number .....	13
1.7 Oberbeck-Boussinesq Approximation.....	13
1.8 Heat Transfer .....	15
1.8.1 Conduction.....	15
1.8.2 Convection .....	15
1.8.3 Radiation .....	15
1.9 Mass Transfer.....	16
1.10 Literature Review.....	16
1.11 Objectives of the Thesis.....	18
1.12 bvp4c.....	18
Chapter 2.....	19
Buoyancy influenced Falkner-Skan slip flow of nanofluids utilizing Tiwari and Das model.....	19
2.1 Introduction.....	19
2.2 Basic Equations and Similarity Solutions using MATLAB Package bvp4c .....	19

2.3 Analysis of Computational Results.....	24
Chapter 3.....	31
Buongiorno model for slip flow past a flat plate with variable free stream velocity.....	31
3.1 Introduction.....	31
3.2 Basic Equations and Similarity Transformations .....	31
3.3 Numerical Results and Discussion.....	34
Chapter 4.....	37
Conclusion and Future Works .....	37
Bibliography .....	39

## *Acknowledgments*

First of all I would like to thank Almighty Allah, the creator of everything, for blessing me and giving me the strength and confidence to accomplish this work.

I would like to convey my heartfelt thanks to my supervisor, **Dr. Meraj Mustafa Hashmi**, for his constant support, inspiration, helpful counselling and invaluable assistance during my thesis. His unwavering commitment to perfection kept me focused. His nice and dedicated behaviour as well as his enthusiastic support was a source of inspiration for me to complete this thesis.

My sincere gratitude is to my GEC members, **Dr. Muhammad Asif Farooq** and **Dr. Mujeeb Ur Rehman** for their guidance and support that helped me in completing this thesis on time.

My heartiest and sincere salutation to my parents and my kids for their patience, great efforts, support and encouragement during this time period.

I would extend my gratitude to my colleagues **Sahreen Tahira, Talat Rafiq, Javaria Aafaq** and **Muhammad Faraz** for their corporation and guidance on various stages during my research work. I would also like to thank my friends for their moral support and prayers.

Lastly, I would like to acknowledge the administration staff as well the helpers at my department for helping me whenever I needed their assistance.

**Ammara Bhatti**



## Abstract

This thesis is concerned with the formation of boundary layer near a flat plate/wedge placed in water-based nanofluids. In model development, partial slip assumption is employed which results in the Robin-type condition in longitudinal velocity component. The resulting heat transfer process with a prescribed surface temperature is also formulated and analysed using thermal slip condition. In this thesis, two well-known theoretical models namely (i) Tiwari and Das model and (ii) Buongiorno model are applied. Firstly, buoyancy assisted or opposed Falkner-Skan flow over a heated static wedge using Tiwari and Das model is formulated. Here, nanoparticle working fluid is assumed to be water based and it contains different nanoparticle materials. The governing problem is transformed in to a coupled self-similar boundary value problem whose numerical solution is developed by MATLAB package *bvp4c* based on the collocation approach. Numerical simulations for velocity and temperature fields are scrutinized for full ranges of solid volume fraction ( $\phi$ ) and pressure gradient parameter ( $m$ ) under both assisting and opposing scenarios. A comparative analysis of wall shear and heat transfer rate is conducted for different nanoparticle materials. The computational results clearly demonstrate that nanofluid assumption is indeed vital for thermal conductivity enhancement of convectational heat transfer fluids. Secondly, Buongiorno's formulation is invoked to model nanofluid transport phenomenon over a flat plate at zero incidence, when a prescribed free stream velocity is considered. Here the unconventional condition of nanoparticle mass flux is treated. Also, variation of diffusion coefficients with temperature is retained and it is concluded that Brownian and thermophoresis diffusions have no effects on the thermal heat transfer.

# Chapter 1

## Introduction

This chapter includes fundamental concepts concerning boundary layer flows and heat transfer. Conservation equations representing boundary layer flows over flat plate and wedge with variable free stream velocity are explained. Dimensionless parameters appearing in this thesis are briefly explained. Two well-known nanofluid models and their attributes are described briefly. This chapter also presents a comprehensive review related to Falkner-Skan flows and nanofluid models. Numerical procedure adopted in the problems is also explained.

### 1.1 Boundary Layer Flow

When a fluid flows over a solid surface, a boundary layer is formed where the relative motion between the fluid particles exists due to significant effects of frictional forces. Fluid in contact with the solid surface at rest has velocity equal to the wall velocity i.e.; zero velocity, due to no-slip condition. The layer of fluid near the surface where frictional effects cannot be neglected is called boundary layer. The flow outside this layer is unaffected by the wall friction and hence it has zero shear stress and moves with the so-called free stream velocity.

In 1904, Ludwig Prandtl introduced boundary layer theory. His work has directed to an entire research community field of study that permits a combination of viscous flow and inviscid flows inside and outside the boundary layers respectively.

Likewise momentum boundary layer, a **thermal boundary layer** also develops when the ambient or bulk temperature and the solid surface temperature differ due to conduction or diffusion. The fluid particle in contact with the surface have the wall temperature and they transfer energy between the fluids layers due to which a temperature gradient develops in the fluid. Thermal boundary layer refers to the zone where temperature gradient is present. (see Fig. 1.1)

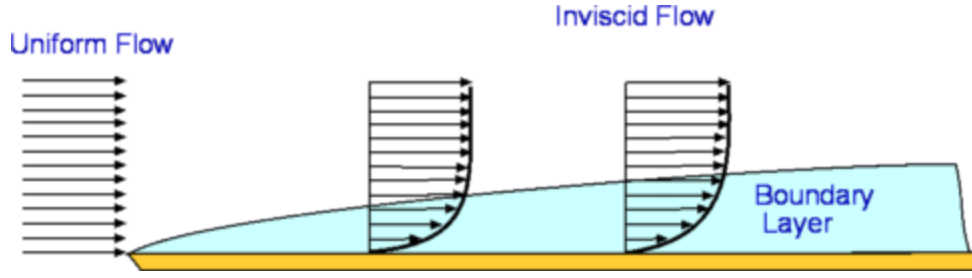


Fig. 1.1: Boundary Layer Flow (source: Internet)

## 1.2 Falkner-Skan Flow

In 1931, Falkner and Skan [1] discovered an interesting family of boundary layer flows. Numerical solution for Falkner-Skan flow was found by Hartree in 1937 [2]. Suppose that fluid motion occurs over a static or moving wedge making an angle  $\beta\pi$  with the horizontal;  $\beta$  being the Hartree parameter that measures the favourable ( $\beta > 0$ ) and unfavorable ( $\beta < 0$ ) pressure gradient (see Fig. 1.2). Assume that the external flow is characterized by  $U(x) = ax^m$ , where  $a$  and  $m$  are constants. Moreover, Hartree parameter  $\beta$  is connected with  $m$  according to the following:

$$\beta = \frac{2m}{m+1}, \quad (1.1)$$

Blasius boundary layer can be generalized by assuming that wedge makes an angle  $\beta\pi/2$  with non-uniform stream velocity  $U(x)$ , In this case, similarity transformations are selected as follows:

$$\eta = \left( \frac{(m+1)U(x)}{2\nu_f x} \right)^{\frac{1}{2}} y, \quad \psi = \left( \frac{2\nu_f x U(x)}{(m+1)} \right)^{\frac{1}{2}} f(\eta), \quad (1.2)$$

$$u = \frac{\partial \psi}{\partial y}, \quad v = -\frac{\partial \psi}{\partial x}.$$

In light of Eq. (1.2), the Navier-stokes equations are transformed as follows:

$$f''' + ff'' + \beta(1 - f'^2) = 0 \quad (1.3)$$

*Special Case:*

For flat plate:  $m = 0$  or  $\beta = 0$ , Eq. (1.3) reduces to:

$$f''' + ff'' = 0 \quad (1.4)$$

which we recognize as Blasius equation, in which free stream velocity  $U, \rho$  and  $\mu$  are kept constant.

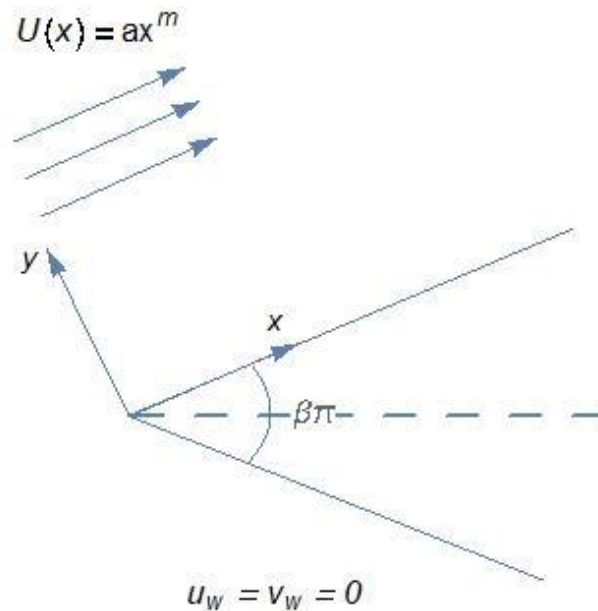


Fig. 1.2: Falkner-Skan flow

### 1.3 Nanofluids

These are novel heat transfer fluids that have much higher thermal conductivity than the conventional coolants. Nanofluid consists of nanoscale particles made up of metals, oxides, ceramics, nitride ceramics and carbide ceramics while water, oil, and ethylene glycol are chosen as common base fluids.

## 1.4 Mathematical Models for Thermal Transport Using Nanofluids

### 1.4.1 Tiwari and Das Model

In this model, nanofluid properties are treated as linear functions of the properties of base fluids and nanoparticles. Equations of continuity, linear momentum and energy are expressed in the following forms:

$$\nabla \cdot \mathbf{V} = 0, \quad (1.5)$$

$$\rho_{nf} \left( \frac{\partial \mathbf{V}}{\partial t} + (\mathbf{V} \cdot \nabla) \mathbf{V} \right) = -\nabla p + \mu_{nf} \nabla^2 \mathbf{V}, \quad (1.6)$$

$$\frac{\partial T}{\partial t} + (\mathbf{V} \cdot \nabla) T = \alpha_{nf} \nabla^2 T, \quad (1.7)$$

where  $\mathbf{V}$  designates the velocity vector and  $T$  stands for local fluid temperature. A model for effective viscosity  $\mu_{nf}$  was suggested by Brinkmann [3]:

$$\mu_{nf} = \frac{\mu_f}{(1 - \phi)^{2.5}}, \quad (1.8)$$

The well accepted expressions for effective density  $\rho_{nf}$ , thermal diffusivity  $\alpha_{nf}$ , effective heat capacity  $(\rho C_p)_{nf}$  and effective thermal expansion co-efficient  $(\rho \beta_1)_{nf}$  are given by Oztop and Abu-Nada [4]:

$$\begin{aligned} \rho_{nf} &= (1 - \phi)\rho_f + \phi\rho_s, \quad \alpha_{nf} = \frac{k_{nf}}{(\rho C_p)_{nf}}, \\ (\rho C_p)_{nf} &= (1 - \phi)(\rho C_p)_f + \phi(\rho C_p)_s, \\ (\rho \beta_1)_{nf} &= (1 - \phi)(\rho \beta_1)_f + \phi(\rho \beta_1)_s, \end{aligned} \quad (1.9)$$

Furthermore, a widely employed expression for thermal conductivity of nanofluids was proposed by Maxwell [5]:

$$k_{nf} = k_f \frac{(k_s + 2k_f) + 2\phi(k_s - k_f)}{(k_s + 2k_f) - \phi(k_s - k_f)}, \quad (1.10)$$

in Eqs. (1.8)-(1.10),  $\phi$  shows nanoparticle volume fraction while subscripts  $f$  and  $s$  are used to signify properties of base fluid and nanoparticle materials respectively.

#### 1.4.2 Buongiorno Model

In 2006, Buongiorno [6] came up with a two component nanofluid transport model comprising four equations. He identified seven mechanisms that can induce relative velocity between nanoparticles and base fluids and argued that only two parameters namely Brownian diffusion and thermophoresis are prominent parameters. Based on this conclusion, he presented the following set of conservation equations:

$$\nabla \cdot \mathbf{V} = 0, \quad (1.11)$$

$$\rho_{nf} \left( \frac{\partial \mathbf{V}}{\partial t} + (\mathbf{V} \cdot \nabla) \mathbf{V} \right) = -\nabla p + \nabla \cdot \boldsymbol{\tau}, \quad (1.12)$$

$$(\rho C_p)_{nf} \left( \frac{\partial T}{\partial t} + (\mathbf{V} \cdot \nabla) T \right) = -\nabla \cdot \mathbf{q} - C_p \mathbf{J}_p \cdot \nabla T, \quad (1.13)$$

$$\left( \frac{\partial \varphi}{\partial t} + (\mathbf{V} \cdot \nabla) \varphi \right) = -\frac{1}{\rho_p} \nabla \cdot \mathbf{J}_p, \quad (1.14)$$

where  $\mathbf{q}$  and  $\mathbf{J}_p$  show heat and mass fluxes respectively. These are expressed as:

$$\mathbf{q} = -k_{nf} \nabla T \quad \mathbf{J}_p = -\rho_p \left( D_B \nabla \varphi + \frac{D_T \nabla T}{T} \right), \quad (1.15)$$

in which  $D_T$  and  $D_B$  represents diffusion coefficients due to thermophoresis and Brownian motion respectively. These are further expressed as  $D_T = C_T \cdot \varphi$  and  $D_B = C_B / T$ . Furthermore,  $\varphi$  stands for nanoparticle concentration. Invoking Eq. (1.15), Eq. (1.13) and Eq. (1.14) becomes:

$$(\rho C_p)_{nf} \left( \frac{\partial T}{\partial t} + (\mathbf{V} \cdot \nabla) T \right) = \nabla \cdot (k_{nf} \nabla T) + C_p \rho_p \left( C_B T \nabla \varphi + C_T \varphi \frac{\nabla T}{T} \right) \cdot \nabla T. \quad (1.16)$$

$$\left( \frac{\partial \varphi}{\partial t} + (\mathbf{V} \cdot \nabla) \varphi \right) = \nabla \cdot \left( C_B T \nabla \varphi + C_T \varphi \frac{\nabla T}{T} \right),$$

## 1.5 Slip and No-slip Boundary Conditions

When the velocity of the fluid is not equal to the velocity of the boundary at the interface or there is some relative motion between the fluid and the wall then the conditions are termed as velocity slip condition. Whereas, the no-slip condition for viscous fluids assumes that the fluid will have zero velocity relative to the boundary at the interface.

## 1.6 Some Dimensionless Numbers

### 1.6.1 Reynolds Number

The ratio between inertial and viscous force is known as Reynolds number. Mathematically, we have

$$Re = \frac{UL}{\nu}, \quad (1.17)$$

where  $L$  denotes the characteristic length,  $U$  shows the free stream velocity and  $\nu$  designates the kinematic viscosity. Laminar and turbulent flow regimes can be distinguished by using the Reynolds number. Laminar flow occurs at low Reynolds numbers where viscous forces are prominent. The flow is turbulent at high Reynolds numbers where inertial forces are dominant.

### 1.6.2 Schmidt Number

The Schmidt number ( $Sc$ ) defines the ratio of momentum diffusivity (kinematic viscosity) to the mass diffusivity. It characterizes flow situations where momentum and mass diffusions are simultaneously occurring. Mathematically, it is given as:

$$Sc = \frac{\nu}{D}, \quad (1.18)$$

### 1.6.2 Prandtl Number

The ratio of momentum diffusion to the thermal diffusion defines the Prandtl number ( $Pr$ ). It is written mathematically as:

$$Pr = \frac{\nu}{\alpha} = \frac{\mu/\rho}{k/\rho C_p} = \frac{\mu C_p}{k}, \quad (1.19)$$

where  $\alpha$  shows the fluid's thermal diffusivity.

### 1.6.3 Grashof Number

The Grashof number, named after Franz Grashof, is a dimensionless number that gives the ratio of buoyant force to the viscous force.

Mathematically,

$$Gr = \frac{\text{buoyant force}}{\text{viscous force}} = \frac{g\beta_1\Delta TL^3}{\nu^2}, \quad (1.20)$$

where,  $\beta_1$  represents the thermal expansion coefficient.

### 1.6.5 Nusselt number

The Nusselt number ( $Nu$ ) characterizes the relative importance of convective to that of conductive heat transfer. Mathematically, it is expressed as:

$$Nu = \frac{hL}{k}, \quad (1.21)$$

where  $L$  shows the characteristic length,  $h$  stands for convective heat transfer coefficient and  $k$  shows fluid thermal conductivity. Nusselt number reflects the dimensionless temperature gradient at the surface of solid.

## 1.7 Oberbeck-Boussinesq Approximation

Oberbeck-Boussinesq approximation is used to deal with flow problems like natural convection. According to this approximation, it is assumed that density variations have a little effect on the flow field other than to cause buoyancy forces. The density of fluid must be a function of the temperature for thermal convection to occur and hence density takes the form:

$$\rho = \rho_o[1 - \beta_1(T - T_o)], \quad (1.22)$$

where  $\rho_o$  is the fluid density at temperature  $T_o$  and  $\beta_1$  is the coefficient of thermal expansion.



In general, for compressible flow, the momentum equation can be expressed as:

$$\rho \left( \frac{\partial \mathbf{V}}{\partial t} + (\mathbf{V} \cdot \nabla) \mathbf{V} \right) = -\nabla p + \nabla \cdot \left( \mu A_1 - \frac{2}{3} \mu (\nabla \cdot \mathbf{V}) \mathbf{I} \right) + \rho \mathbf{g}, \quad (1.23)$$

where  $A_1 = (\nabla \mathbf{V} + (\nabla \mathbf{V})^T)$  is the strain rate tensor,  $\mathbf{V}$  is the fluid velocity,  $\rho$  is the density,  $p$  is the pressure,  $\mu$  is the dynamic viscosity of the fluid,  $\mathbf{I}$  is the identity matrix, and  $\mathbf{g}$  is the acceleration due to gravity.

The continuity equation for compressible fluid is  $\frac{1}{\rho} \frac{d\rho}{dt} + \nabla \cdot \mathbf{V} = 0$ .

According to the Oberbeck-Boussinesq approximation, density variation is only significant in the buoyancy factor  $\rho \mathbf{g}$ , and it can be ignored in the rest of the equation. This result (1.23) in:

$$\rho_o \left( \frac{\partial \mathbf{V}}{\partial t} + (\mathbf{V} \cdot \nabla) \mathbf{V} \right) = -\nabla p + \nabla \cdot \left( \mu A_1 - \frac{2}{3} \mu (\nabla \cdot \mathbf{V}) \mathbf{I} \right) + \rho \mathbf{g}, \quad (1.24)$$

Except in the body force term expressing the buoyancy force, the temperature and pressure-dependent density  $\rho$ , has been replaced with a constant density  $\rho_o$ .

Since the magnitude of  $\frac{1}{\rho} \frac{d\rho}{dt}$  is small compared with the term  $\nabla \cdot \mathbf{V}$ , the continuity equation

$\frac{1}{\rho} \frac{d\rho}{dt} + \nabla \cdot \mathbf{V} = 0$ , reduces to the incompressible form  $\nabla \cdot \mathbf{V} = 0$  under the Boussinesq

approximation. As a result, the term  $\frac{2}{3} \mu (\nabla \cdot \mathbf{V}) \mathbf{I}$  in the Navier-Stokes equations is zero as well.

The viscosity  $\mu$ , is also commonly believed to be constant. As a result, the diffusion term

$\nabla \cdot (\mu (\nabla \mathbf{V} + (\nabla \mathbf{V})^T))$  can be recast as  $\mu \nabla^2 \mathbf{V}$ . By using these above assumptions, equation (1.24)

can be written as follows:

$$\rho_o \left( \frac{\partial \mathbf{V}}{\partial t} + (\mathbf{V} \cdot \nabla) \mathbf{V} \right) = -\nabla p + \mu \nabla^2 \mathbf{V} + \rho \mathbf{g}, \quad (1.25)$$

The buoyancy term  $\rho \mathbf{g}$  can also be stated as  $\rho_o \mathbf{g} - \rho_o \beta_1 (T - T_0) \mathbf{g}$  in view of equation (1.22). So the equation for conservation of momentum becomes:

$$\rho_o \left( \frac{\partial \mathbf{V}}{\partial t} + (\mathbf{V} \cdot \nabla) \mathbf{V} \right) = -\nabla (p - \rho_o \mathbf{g} \cdot \mathbf{z}) + \mu \nabla^2 \mathbf{V} - \rho_o \beta_1 (T - T_0) \mathbf{g}. \quad (1.26)$$

## 1.8 Heat Transfer

The thermal flow of energy between physical systems is known as heat transfer. Heat transmission is possible if there is a temperature difference between two physical systems. Heat can be transferred across systems in three ways: radiation, convection, and conduction.

### 1.8.1 Conduction

The process of heat transfer caused by molecule collisions is known as conduction. Heat conduction, electrical conduction, and sound conduction are all terms that are frequently used to describe three different types of activity. Fourier proposed that the rate of heat transfer per unit area is proportional to the temperature gradient, i.e.,

$$\frac{Q}{A} = -k \frac{dT}{dx}, \quad (1.27)$$

where  $k$  is the proportionality constant known as thermal conductivity,  $A$  is the area,  $Q$  is the heat transfer rate and  $\frac{dT}{dx}$  is the temperature gradient in the preceding equation.

### 1.8.2 Convection

Convection is the movement of fluid particles from a location of high thermal energy to a region of low thermal energy. It is the energy transfer caused by bulk fluid motion in fluid dynamics. The nature of convective heat transmission is determined by the flow. As a result, there are three types of convection: Natural (free) convection, Forced convection and mixed convection. Heat transfer mechanism given by Newton's law of cooling as

$$\frac{Q}{A} = h(T_w - T_f), \quad (1.28)$$

in which  $T_w$  shows wall temperature whereas  $T_f$  is surrounding temperature characterized by heat transfer coefficient  $h$ .

### 1.8.3 Radiation

In the infrared and visible portions of the electromagnetic spectrum, radiation is the transfer of thermal energy carried by photons of light. Radiation is a mechanism by which all bodies constantly emit thermal energy. It can be sent without the use of any medium.

## 1.9 Mass Transfer

Mass transfer refers to the movement of chemical species from one location to another as a result of a concentration gradient. Diffusion is the same as conduction when it comes to mass transfer. Heat and mass transport are both kinetic processes that can be investigated independently or together. It is more efficient to couple heat and mass transfer equations in the case of diffusion-convection phenomena.

## 1.10 Literature Review

Falkner-Skan model, discovered decades ago by Falkner and Skan [1], has central importance in fluid dynamics of wall-bounded flows. It is characterized by a laminar boundary layer formed on a wedge in the existence of an external free stream velocity  $U(x) \propto x^m$ . The authors in [1] proposed a transformation technique that yields flow problem involving a parameter  $\beta = 2m/(m + 1)$ , measuring the adverse or favorable pressure gradient. Some approximate procedures were adopted for analysing the self-similar system in [1]. Later, Hartree [2] came up with a numerical approximation of self-similar Falkner-Skan equation using shooting method. More detailed analysis of the Falkner-Skan equation was provided by Stewartson [7] who found a lower bound  $\beta_c$  of  $\beta$ , beyond which the solution does not exist. He also discovered that dual solutions exist in the range  $\beta_c < \beta < 0$ . Yang and Chein [8] reported unique analytic solutions comprising of hyper geometric functions, for Falkner-Skan model when  $\beta = -1$ . Brauner *et al.* [9] later showed that Falkner-Skan equation with  $\beta = -1$  can be reduced to the Riccati equation. Owing to its theoretical significance, a considerable research concerning Falkner-Skan flow under different situations is published to date. Local similarity solutions for visco-elastic Falkner-Skan flow were found by Rajagopal *et al.* [10] utilizing second-grade model. Their results predicted the contribution of elastic effects on the pressure gradient driven flow adjacent a wedge. Later, the contribution of surface porosity on the boundary layer was numerically studied by Watanabe [11]. Yih [12] investigated self-similar PDEs representing forced convection heat transfer over a porous wedge with suction or blowing using Keller-Box numerical scheme. Asaithambi [13] applied a finite difference technique to deal with the Falkner-Skan model, by transforming the semi-infinite physical domain to the unit interval  $[0,1]$ . The author indicated that the computational effort required by finite difference approach is considerably less in

comparison to the Newton method based shooting algorithm. Falkner-Skan model with viscoelastic fluid governed by FENE-P constitutive equation was treated numerically by Olagunju [14]. Author showed that self-similar solution is achievable only when  $m = 1/3$  is chosen. Yacob et al. [15] formulated Falkner-Skan motion by considering nanoparticle working fluid and studied the consequences of solid volume fraction on resulting heat transfer for various nanoparticle materials. Quite recently, closed form analytical results for Falkner-Skan flow and accompanying heat transfer were developed by Fang et al. [16] in a special case where  $\beta = -1$ . Further studies featuring Falkner-Skan flows under different scenarios include those published by Hayat et al. [17], Turkyilmazoglu [18], Merkin [19], Das et al. [20], Dinarvand [21], Awaludin et al. [22], and Wang [23].

Nanotechnology has been largely adopted in industries since materials with nanoscale sizes exhibit distinct chemical and physical properties. A relatively new class of fluids containing emulsions or suspensions of nanostructures (such as fibers, tubes, particles, droplets) in fluid media (water, ethylene glycol etc.), are termed nanofluids. Eastman et al. [24] discovered that thermal conductivity of ethylene glycol fluid rises up to 40% when only 0.3% volume fraction of copper particles with diameter  $<10$  nm are dispersed in it. Several unique applications of such fluids, requiring rapid and efficient heat transfer have been identified. Also, various interesting review articles outlining remarkable applications of such fluids in solar power technology, in microelectronics, in large scale cooling, in biomedicine, in machining and in transportation are published (see, for instance [25]-[27] and articles there in). A frequently adopted mathematical model was introduced by Buongiorno [6] in 2006 that considers the contributions of Brownian diffusion and thermophoresis in transport equations. Buongiorno's approach was initially followed in a series of papers by Nield and Kuznetov [28]-[32] dealing with natural convection along a flat plate embedded in nanofluid. In these papers, the diffusions were assumed to be constant and temperature differences were assumed sufficiently small. It was later reported by Myers et al. [33], the Buongiorno's framework was not accurately reported by many studies including the ones cited above. They noticed that both Brownian diffusion and thermophoresis effects do not alter the heat transfer performance of a nanoparticle working fluid, which is quite opposite to what has been claimed in several past papers. Formulation proposed in [6] has been adopted in many other papers to examine a wide variety of flow models (see refs. [34]-[37] and articles there in). Tiwari and Das [38] put forward a single-phase model for nanofluid thermal

transport, in which thermo physical properties of resulting nanofluid were expressed as linear combinations of properties of base fluid and its constituents. This model was utilized in numerous articles to explore nanofluid insights in well-known boundary layer flows (see refs. [39]-[42] and articles there in).

### **1.11 Objectives of the Thesis**

Motivation of current thesis is twofold. Firstly to consider buoyancy effects in Falkner-Skan flow of water based nanofluids under partial slip boundary conditions. Here, for the first time, buoyancy force term for Falkner-Skan flow of nanofluid is formulated using Tiwari and Das model [39]. To preserve self-similarity in the arising system, it is further assumed that wedge surface temperature is proportional to  $x^{2m-1}$ . Contribution of nanoparticle volume fraction towards heat transfer enhancement in Falkner-Skan flow is scrutinized via detailed numerical results. Notably, the aforementioned problems reduce to the classical Blasius flow model of flat plate at zero incidence when  $m = 0$ .

Secondly, the two phase Buongiorno model is implemented to analyse slip flow past a flat plate with variable free stream velocity. Numerical simulations are executed via MATLAB routine `bvp4c`, which has been widely employed these days for the similar boundary layer flows.

### **1.12 `bvp4c`**

Flows occurring in physical world are governed by complex non-linear partial differential equations. These equations may have no solution, have a finite number, or may have infinitely many solutions. In order to get MATLAB programs require the user to provide with the initial guesses for the solution required and also for the parameters involved in the governing equations. A nonlinear multipoint boundary value problem can be solved using a built-in function in MATLAB that is based on collocation approach. Third order differential equations are reduced to first order ordinary differential equations in order to use this approach. For more accurate results, the guesses are offered. Changes in step size can be adjusted to improve accuracy.

## Chapter 2

### **Buoyancy influenced Falkner-Skan slip flow of nanofluids utilizing Tiwari and Das model**

#### **2.1 Introduction**

The study of heat transport and boundary layer flow of water based nanofluids over a heated static wedge under partial slip boundary conditions is covered in this chapter. To preserve self-similarity in the arising system, it is further supposed that temperature of wedge surface is proportional to  $x^{2m-1}$ . The controlling system of partial differential equations (PDEs) is transformed into a system of nonlinear ordinary differential equations (ODEs) using similarity transformation, and then numerically solved using the MATLAB bvp4c function. The numerical values for the wall shear stress and Nusselt number, as well as velocity and temperature, are presented in graphs and tables. Graphs and tables in Section (2.4) illustrate the effects of various parameters on flow and heat transfer characteristics.

#### **2.2 Basic Equations and Similarity Solutions using MATLAB Package bvp4c**

Consider the Falkner-Skan flow situation (illustrated in Fig. 1), that involves water based nanofluids along a heated wedge making an angle  $\beta\pi/2$  with the horizontal. We treat the case of static wedge where pressure gradient is applied to achieve a prescribed free stream velocity  $U(x) = ax^m$ , where  $a > 0$  is a constant. Let  $u$  and  $v$  designate velocities along the  $x$  – and  $y$  – directions where coordinate  $x$  extends along the wedge surface and  $y$  is normal to it. Unlike most of the past studies, present work retains the contribution of buoyancy force term on the resulting flow phenomena. In addition, partial slip assumption is invoked that leads to Robin-type condition for both tangential velocity and temperature. Tiwari and Das formulation will be implemented to seek how solid volume fraction of four different kinds of nanoparticle materials (namely copper (Cu), alumina ( $Al_2O_3$ ), copper-oxide (CuO) and titania ( $TiO_2$ )), affects the flow field. In this case, a prescribed surface temperature distribution is assumed which ensures that developed problem admits a self-similar solution. Invoking the Oberbeck-Boussinesq approximation and Tiwari and Das nanofluid model [38] as well as the Bernoulli's equation in

free stream, the governing non-linear PDEs of mass, momentum and energy can be written as follows:

$$\frac{\partial u}{\partial x} + \frac{\partial v}{\partial y} = 0, \quad (2.1)$$

$$u \frac{\partial u}{\partial x} + v \frac{\partial u}{\partial y} = U \frac{dU}{dx} + \nu_{nf} \left( \frac{\partial^2 u}{\partial y^2} \right) + g \frac{(\rho\beta_1)_{nf}}{\rho_{nf}} (T - T_\infty) \sin\left(\frac{\beta\pi}{2}\right), \quad (2.2)$$

$$\left( u \frac{\partial T}{\partial x} + v \frac{\partial T}{\partial y} \right) = \frac{k_{nf}}{(\rho c_p)_{nf}} \frac{\partial^2 T}{\partial y^2}, \quad (2.3)$$

where  $\nu_{nf}$ ,  $\rho_{nf}$ ,  $k_{nf}$ ,  $(\rho c_p)_{nf}$  and  $\beta_1$  represents the effective kinematic viscosity, effective density, effective thermal conductivity, effective heat capacity, and co-efficient of thermal expansion respectively. Table 2.1 shows theoretical models for these quantities, whereas thermo-physical properties of water and nanoparticles are listed in table 2.2.

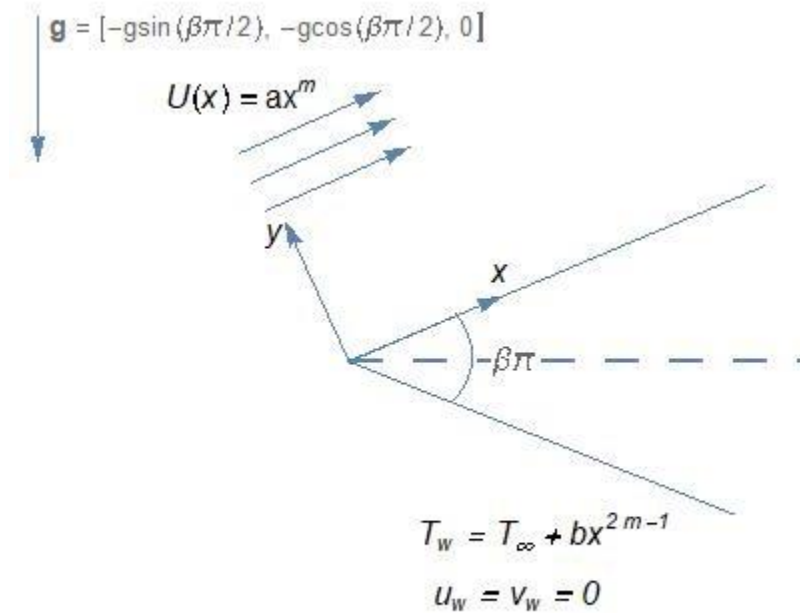


Fig. 2.1: Physical representation and coordinate system

**Table 2.1:** Effective thermo physical properties of nanofluids where subscripts  $f, nf$  and  $s$  relate to fluid, nanofluid and nanoparticles respectively (Oztop and Abu-Nada [4]).

Properties	Models
Dynamic viscosity ( $\mu_{nf}$ )	$\mu_{nf} = \frac{\mu_f}{(1 - \phi)^{2.5}}$
Kinematic viscosity ( $\nu_{nf}$ )	$\nu_{nf} = \frac{\nu_f}{(1 - \phi)^{2.5} ((1 - \phi)\rho_f + \phi\rho_s)}$
Density ( $\rho_{nf}$ )	$\rho_{nf} = (1 - \phi)\rho_f + \phi\rho_s$
Heat capacity ( $(\rho C_p)_{nf}$ )	$(\rho C_p)_{nf} = (1 - \phi)(\rho C_p)_f + \phi(\rho C_p)_s$
Thermal conductivity ( $k_{nf}$ )	$k_{nf} = k_f \frac{(k_s + 2k_f) - 2\phi(k_f - k_s)}{(k_s + 2k_f) + \phi(k_f - k_s)}$
Thermal diffusivity ( $\alpha_{nf}$ )	$\alpha_{nf} = \frac{k_{nf}}{(\rho C_p)_{nf}}$
Buoyancy co-efficient ( $(\rho\beta_1)_{nf}$ )	$(\rho\beta_1)_{nf} = (1 - \phi)(\rho\beta_1)_f + \phi(\rho\beta_1)_s$

**Table 2.2:** Thermo physical properties of base fluids and nanoparticles [4].

Property	Base fluid (H <sub>2</sub> O)	Cu	Al <sub>2</sub> O <sub>3</sub>	TiO <sub>2</sub>	CuO
$C_p [L^2T^{-2}\Theta^{-1}]$	4179	385	765	4179	531.8
$\kappa [MLT^{-3}\Theta^{-1}]$	0.613	400	40	8.954	76.50
$\rho [ML^{-3}]$	997.1	8933	3970	4250	6320
$\beta_1 \cdot 10^{-5} [\Theta^{-1}]$	21	1.67	0.85	0.9	0.85

The flow problem is subjected to the following slip boundary conditions:

$$u = N(x)\mu_{nf} \frac{\partial u}{\partial y}, \quad v = 0, \quad T = T_w + D_1(x) \frac{\partial T}{\partial y} \quad \text{at } y = 0, \quad (2.4)$$

$$u \rightarrow U, \quad T \rightarrow T_\infty \quad \text{as } y \rightarrow \infty,$$

where,  $u$  and  $v$  represents the velocity components along the  $x$  – and  $y$  –directions respectively.  $N(x) = N^*(x/U(x))^{1/2}$  and  $D_1(x) = D^*(x/U(x))^{1/2}$  are variable velocity and thermal slip factors respectively.

In order to reduce the Eqs. (2.1) - (2.3) into ODEs, following similarity transformation variables are used [43]:

$$\eta = \left( \frac{(m+1)U(x)}{2\nu_f x} \right)^{1/2} y, \quad \psi = \left( \frac{2\nu_f x U(x)}{(m+1)} \right)^{1/2} f(\eta), \quad \theta(\eta) = \frac{T - T_\infty}{T_w - T_\infty}, \quad (2.5)$$



where  $\psi$  is the dimensional stream function and is expressed in the usual form as  $u = \partial\psi/\partial y$  and  $v = -\partial\psi/\partial x$ ,  $\theta$  is the dimensionless temperature distribution of the nanofluid,  $f$  is the dimensionless stream function and  $\eta$  is independent similarity variable.

By substituting Eq. (2.5) into governing non-linear PDEs (2.2) and (2.3), give us a following set of dimensionless non-linear ODEs:

$$\frac{1}{\epsilon_1} f'''' + f f'' + \frac{2m}{m+1} (1 - f'^2) + \frac{2}{m+1} \frac{\epsilon_2}{\epsilon_3} \theta \lambda \sin\left(\frac{\beta\pi}{2}\right) = 0, \quad (2.6)$$

$$\frac{1}{Pr} \frac{k_{nf}}{k_f \cdot \epsilon_4} \theta'' + \theta' f - \frac{\theta f'}{m+1} (4m-2) = 0, \quad (2.7)$$

where,

$$\epsilon_1 = (1 - \phi)^{2.5} \left\{ (1 - \phi) + \phi \frac{\rho_s}{\rho_f} \right\}, \quad \epsilon_2 = (1 - \phi) + \phi \frac{(\rho\beta_1)_s}{(\rho\beta_1)_f}, \quad \epsilon_3 = (1 - \phi) + \phi \frac{\rho_s}{\rho_f},$$

$$\epsilon_4 = (1 - \phi) + \phi \frac{(\rho c_p)_s}{(\rho c_p)_f}.$$

In Eqs. (2.6) and (2.7),  $Pr = \nu_f (\rho c_p)_f / k_f$  represents base fluid Prandlt number,  $\beta = 2m/m+1$  represents Hartree pressure gradient parameter and  $\lambda = g b (\beta_1)_f / a^2 = Gr_x / (Re_x)^2$  represents the mixed convection parameter in which  $Gr_x = g \beta_f (T_w - T_\infty) x^3 / \nu^2$  and  $Re_x = Ux/\nu$  denote the Grashof and Reynolds number respectively. Furthermore, we notice that  $\lambda$  is a constant, with  $\lambda < 0$  corresponds to opposing flow and  $\lambda > 0$  corresponds to assisting flow, while  $\lambda = 0$  represents the case when buoyancy force is absent (forced convection).

The boundary conditions (2.4) transform to:

$$f(0) = 0, \quad \alpha_1 (1 - \phi)^{-2.5} (m+1)^{\frac{1}{2}} f''(0) = f'(0),$$

$$1 + \gamma (m+1)^{\frac{1}{2}} \theta'(0) = \theta(0) \quad \text{at } \eta = 0, \quad (2.8)$$

$$f' \rightarrow 1, \quad \theta \rightarrow 0 \quad \text{as } \eta \rightarrow \infty.$$

where  $\alpha_1$  and  $\gamma$  are termed velocity and thermal slip parameters. These are defined below:

$$\alpha_1 = N^* \left( \frac{1}{2\nu_f} \right)^{1/2} \mu_f, \quad \gamma = D^* \left( \frac{1}{2\nu_f} \right)^{\frac{1}{2}}. \quad (2.9)$$

In Eq. (2.9),  $\alpha_1$  and  $\gamma$  is the velocity slip parameter and thermal slip parameter respectively.

Shear stress encountered at the wall is evaluated as follow:

$$\tau_w = \mu_{nf} \left( \frac{\partial u}{\partial y} \right)_{y=0} = \frac{\mu_f}{(1-\phi)^{2.5}} U(x) f''(0) \left( \frac{(m+1)U(x)}{2\nu_f x} \right)^{\frac{1}{2}}. \quad (2.10)$$

Eq. (2.10) can be used to evaluate the skin friction coefficient  $C_f = \tau_w / \rho_f U^2(x)$ :

$$(Re_x)^{1/2} C_f = \left( \frac{m+1}{2} \right)^{1/2} \frac{f''(0)}{(1-\phi)^{2.5}}, \quad (2.11)$$

where  $Re_x = Ux/\nu_f$  defines the local Reynolds number.

Defining the local Nusselt number  $Nu_x = xq_w/k_{nf}(T_w - T_\infty)$  with  $q_w = -k_{nf}(\partial T/\partial y)_{y=0}$  representing heat flux at the surface, we reach the following result:

$$(Re_x)^{-1/2} Nu_x = - \left( \frac{m+1}{2} \right)^{1/2} \theta'(0). \quad (2.12)$$

To discover physical insights in the present model, Eqs. (2.11) and (2.12) clearly show that one must focus on the values of  $f''(0)$  and  $\theta'(0)$ .

For the solution of boundary-value problem comprising Eqs. (2.6) and (2.7) together with conditions (2.8), an easy to apply yet reliable package `bvp4c` of MATLAB is used. By using the following substitution:

$$y_1 = f, \quad y_2 = f', \quad y_3 = f'', \quad y_4 = \theta \quad \text{and} \quad y_5 = \theta', \quad (2.13)$$

the equivalent first-order system is found given below:

$$y_1' = y_2, \quad (2.14)$$

$$y_2' = y_3, \quad (2.15)$$

$$y_3' = -\epsilon_1 \left\{ y_1 y_3 + \frac{2m}{m+1} (1 - y_2^2) + \frac{2}{m+1} \frac{\epsilon_2}{\epsilon_3} \theta \lambda \sin \left( \frac{\beta\pi}{2} \right) \right\}, \quad (2.16)$$

$$y_4' = y_5, \quad (2.17)$$

$$y_5' = Pr\epsilon_4 \frac{k_f}{k_{nf}} \left\{ \frac{y_4 y_2}{m+1} (4m-2) - y_5 y_1 \right\}. \quad (2.18)$$

Eqs. (2.14)-(2.18) are solved by bvp4c routine that applies collocation approach which yields C1-continuous polynomial valid in the domain of interest. In table 2.3, present code is validated by comparing the data of  $f''(0)$  with the existing studies and such comparison appears excellent.

**Table 2.3:** Effect of pressure gradient parameter  $m$  on wall shear stress  $f''(0)$  when  $\phi = 0$ . A comparison of results with the existing papers.

m	$f''(0)$					
	Rosenhead [44]	Watanabe [11]	Yih et al. [12]	Yacob et al. [15]	Dinarvand [21]	Present results
0		0.46960	0.469600	0.4696	0.469600	0.469600
1/11		0.65498	0.654979	0.6550	0.654993	0.654994
0.2		0.80213	0.802125	0.8021	0.802125	0.802126
1/3		0.92765	0.927653	0.9277	0.927680	0.927680
0.5		1.03890		1.0389	1.038903	1.038900
1	1.232588		1.232588	1.2326	1.232587	1.232590

## 2.3 Analysis of Computational Results

In this section boundary value problem comprising equations (2.6) and (2.7) along with the condition (2.8) have been dealt with the above mentioned procedure. The computational results are utilized to explore the velocity and temperature curves under different controlling parameters. Numerical data of  $f''(0)$  is generated at different  $m$ -values in the special case where  $\phi = \lambda = 0$ . These results appear in perfect match with the corresponding data found by previous authors. Having ascertained the validity of MATLAB code, we now divert our attention to the discussion concerning physical intuition of the model. Figs. (2.2)-(2.12) correspond to the numerical solutions of Eqs. (2.6) and (2.7) formulated under Tiwari and Das model.

Fig. 2.2 include profile of  $f'(\eta)$  representing  $u$ -component velocity profile for different values of  $m$ , measuring the favorable pressure gradient. By increasing parameter  $m$ , the pressure gradient enlarges due to which flow parallel to the wedge accelerates. It is also evident that it requires a lower value of  $y$  for the velocity profile to achieve its free stream condition, when

larger value of  $m$  is selected. This illustrates that boundary layer thickness is suppressed by increasing the pressure gradient. It is notice that deviation in the profiles corresponding to opposing flow is more pronounced when compared with assisting flow situation  $\lambda = 1$ .

Fig. 2.3 include  $\theta$ -curves for different choices of  $m$  under both assisting and opposing flow scenarios. Clearly thermal boundary becomes thinner for increasing  $m$  values. This predicts that the heat transfer rate from the boundary is an increasing function of parameter  $m$ .

Fig. 2.4 scrutinizes the role of buoyancy force on the Falkner-Skan flow with nanoparticles, we compute  $u$  –velocity and temperature profiles by changing the values of  $\lambda$ , the mixed convection parameter. For positive values of  $\lambda$ , buoyancy force serves as favorable pressure gradient its effect is therefore similar to that of  $m$  in qualitative sense. It is revealed that transverse velocity component  $v$  has an increasing relationship with parameter  $\lambda$ .

Fig. 2.5 is generated for see the consequences of buoyancy force term on the temperature profile with and without nanofluid assumption. For increasing  $\lambda$ -values transverse velocity component  $v$  enlarges due to which higher amount of cold fluid is being drawn towards the hot wedge surface. This leads to the thinning of thermal boundary layer as apparent from Fig 2.4. The effect of  $\lambda$  on temperature profiles is relatively less compared to the velocity profiles because this parameter does not appear directly in the similarity energy equation. Moreover, a clear rise in thermal boundary layer thickness becomes evident due to the consideration of nanoparticles.

The curves of velocity field  $f'(\eta)$  obtained by varying velocity slip parameter  $\alpha_1$  are portrait in Fig. 2.6. At the wedge surface, the tangential velocity component  $u$  relates to the shear stress encountered due to the consideration of slip boundary condition. Resultantly by increasing slip coefficient, shear stress at the wall is lowered which leads to a decrease in  $f''(0)$ . This in turn enhances the graph of  $f'$  as noted from Fig. 2.6. Such behavior is qualitatively similar for both positive and negative values of parameter  $\lambda$ .

Fig. 2.7 convey that for both assisting and opposing flow the temperature profile decreases with the increase of thermal slip parameter  $\gamma$ . It is due to the fact that when the  $\gamma$  increases, it reduces frictional heat between nanofluid and the wedge surface. Consequently, the temperature reduces in the boundary layer region and the thermal boundary layer thickness decreases.

In Fig. 2.8, we investigate how temperature curve  $\theta$  is affected by the presence of nanoparticles (Cu). The graph of effective thermal conductivity  $k_{nf}$  versus volume fraction  $\phi$  shows the linear growth in  $k_{nf}$  with  $\phi$ . For such reason thermal boundary layer thickness elevates whenever nanoparticle working fluid is considered.

Fig. 2.9 displays the curves of skin friction coefficient (represented by  $C_f(Re_x^{1/2})$ ) against  $m$  for wide variety of mixed convection parameter. Interestingly, for sufficiently higher values of  $\lambda$ , almost a linear growth in skin friction coefficient with  $m$  is evident. Fig. 2.10 presents the profiles of local Nusselt number as functions of  $m$  for various values of Prandtl number  $Pr$ . For increasing  $Pr$ -values, heat convection becomes stronger compared to pure conduction which results in higher value of wall temperature gradient. Also, heat transfer rate vanishes when  $Pr \rightarrow 0$ .

Figs. 2.11 and 2.12 portray the contribution of solid volume fraction  $\phi$  on skin friction factor and local Nusselt number respectively. Here computations are worked out for four different nanoparticle materials. The Brinkman model [3] of viscosity signifies a direct relationship between the dynamic viscosity  $\mu_{nf}$  and  $\phi$ . Consequently, with an enlargement of  $\phi$ , the skin friction coefficient grows (in non-linear fashion). Furthermore, highest and least values of skin friction factor/local Nusselt number occur, respectively, for copper-Cu and alumina- $Al_2O_3$  nanoparticles.

In table 2.4, the numerical data for  $f''(0)$  and  $\theta'(0)$  is assessed by changing the mixed convection parameter  $\lambda$ , the velocity slip parameter  $\alpha_1$  and nanoparticle volume fraction  $\phi$ . Heat transfer rate grows upon increasing the strength of buoyancy force. Furthermore, a considerable reduction in heat transfer rate is found whenever nanofluid assumption is incorporated. It is natural to notice an augmentation in skin friction coefficient due to the inclusion of nanoparticles.

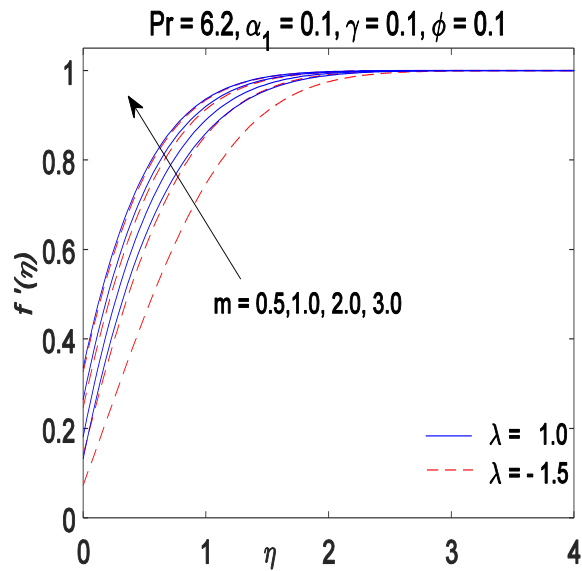


Fig. 2.2: Variation in velocity profile  $f'(\eta)$  with  $\eta$  for different choices of  $m$ .

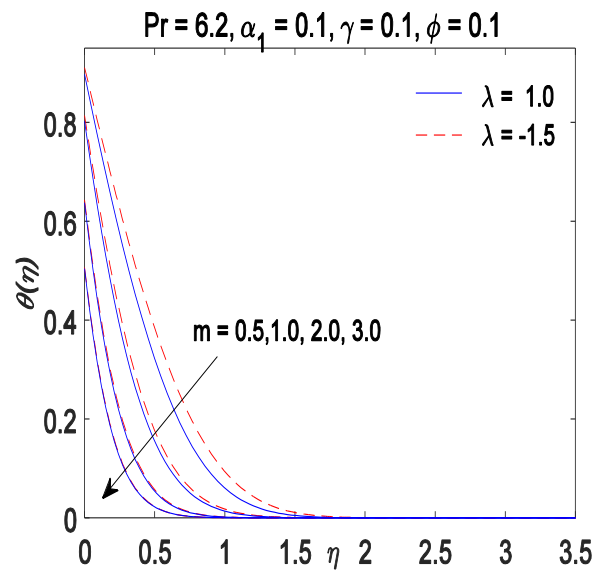


Fig. 2.3: Variation in temperature profile  $\theta(\eta)$  with  $\eta$  for different choices of  $m$ .

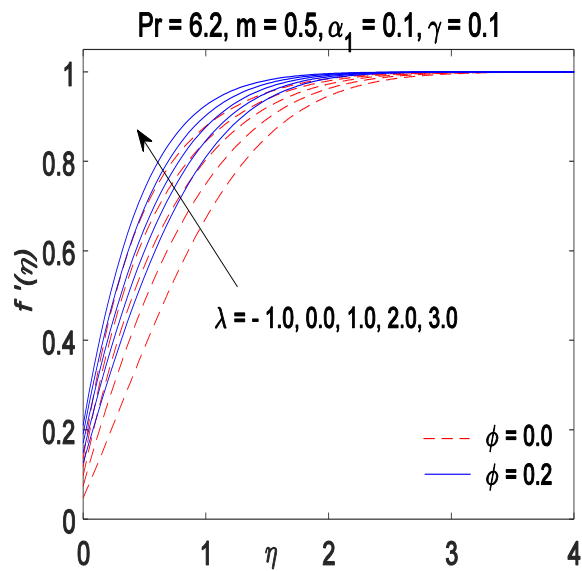


Fig. 2.4: Variation in velocity profile  $f'(\eta)$  with  $\eta$  for different choices of  $\lambda$ .

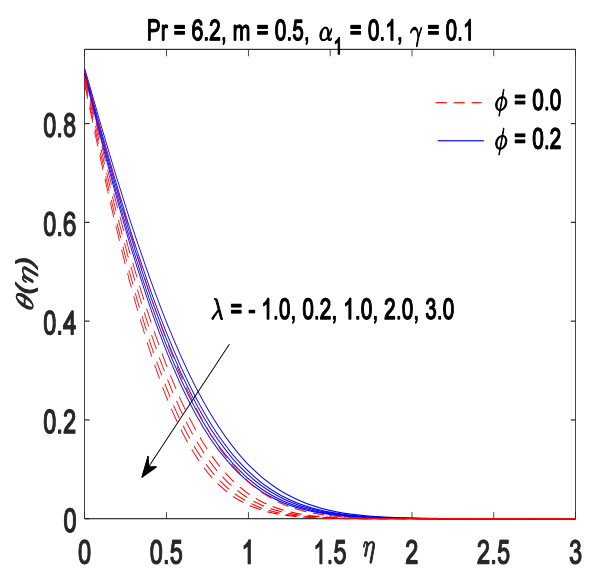


Fig. 2.5: Variation in temperature profile  $\theta(\eta)$  with  $\eta$  for different choices of  $\lambda$ .

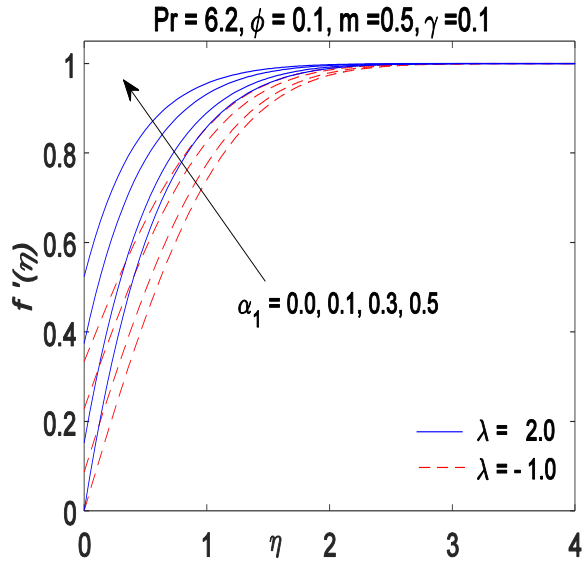


Fig. 2.6: Variation in velocity profile  $f'(\eta)$  with  $\eta$  for different choices of  $\alpha_1$ .

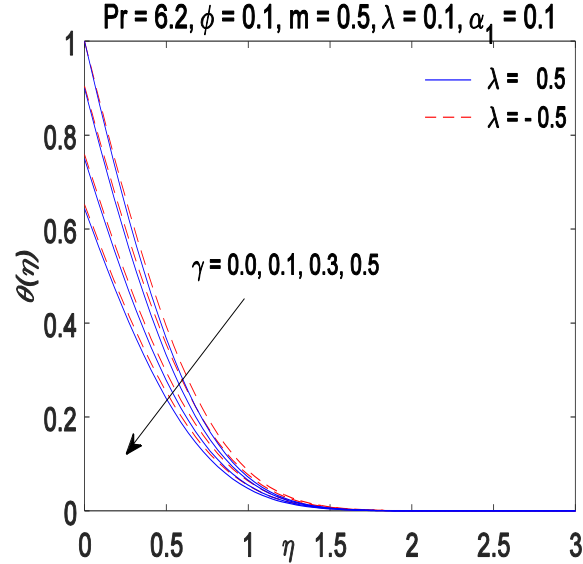


Fig. 2.7: Variation in temperature profile  $\theta(\eta)$  with  $\eta$  for different choices of  $\gamma$ .

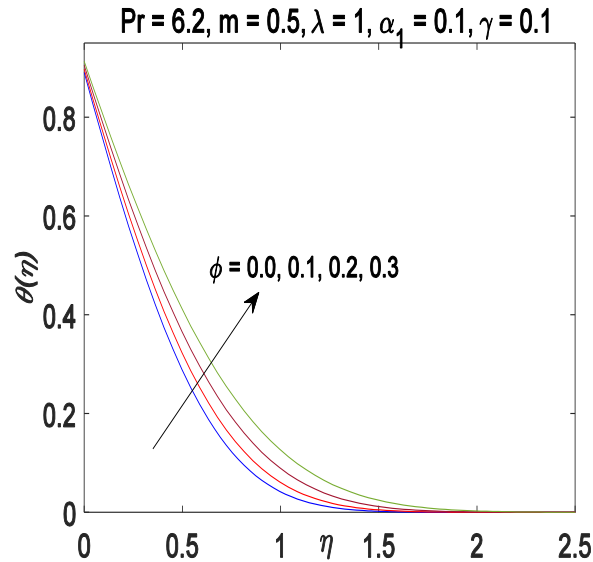


Fig. 2.8: Variation in temperature profile  $\theta(\eta)$  with  $\eta$  for different choices of  $\phi$ .

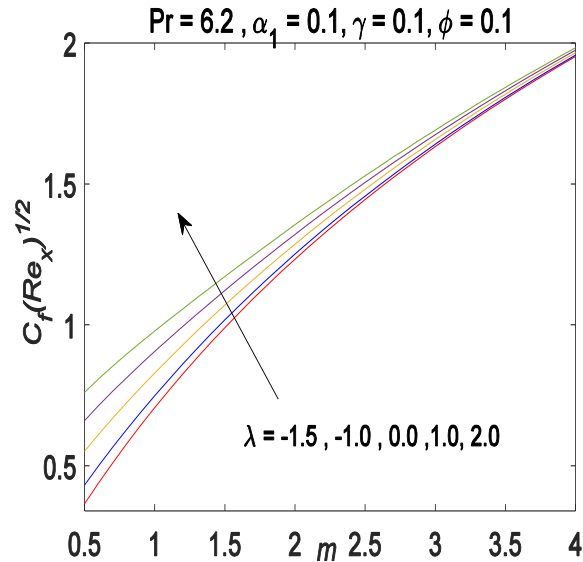


Fig. 2.9: Variation in skin friction coefficient with  $m$  for different values of  $\lambda$ .

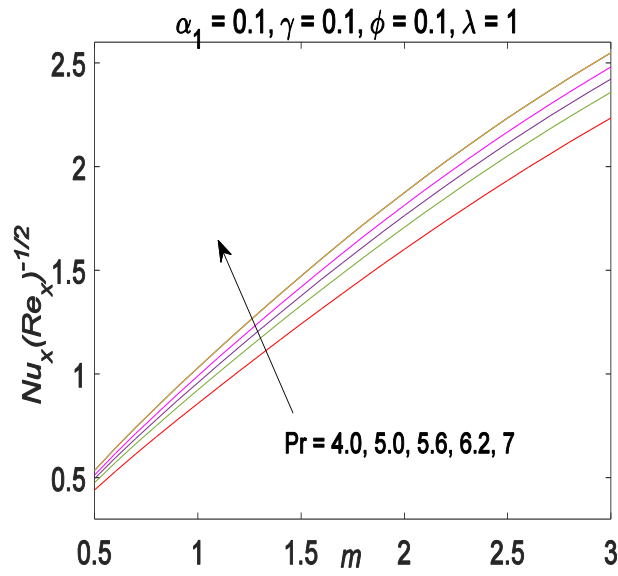


Fig. 2.10: Variation in local Nusselt number with  $m$  for different values of  $Pr$ .

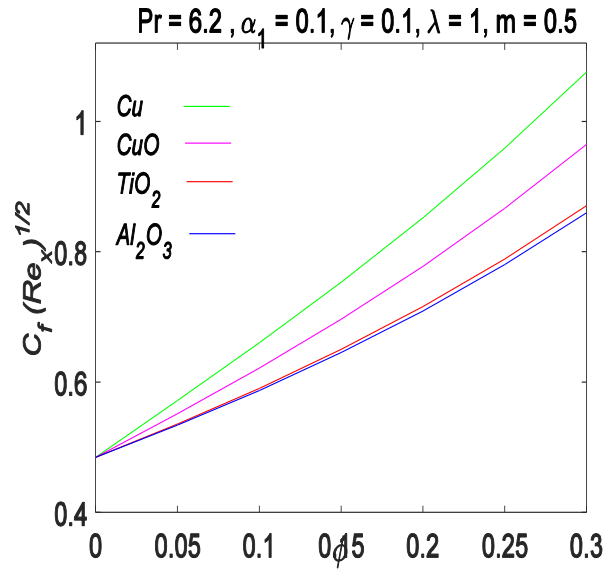


Fig. 2.11: Variation in skin friction coefficient with  $\phi$  for different types of nanoparticles.

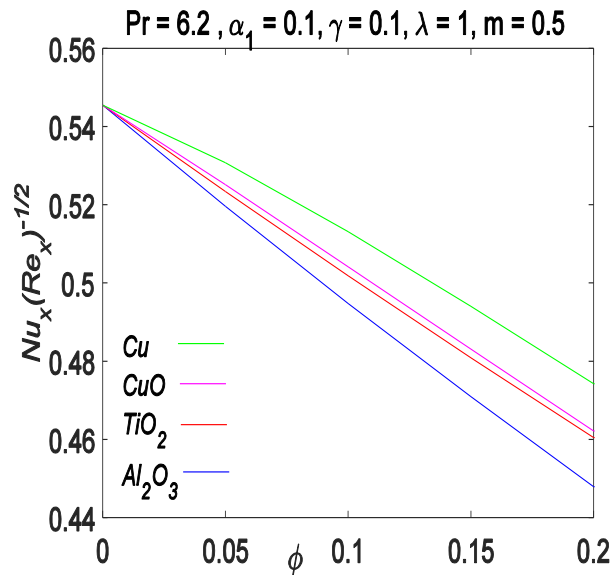


Fig. 2.12: Variation in local Nusselt number with  $\phi$  for different types of nanoparticles.



**Table 2.4:** Numerical data of skin friction coefficient  $f''(0)/(1-\phi)^{2.5}$  and local Nusselt number  $-\theta'(0)$  for different sets of mixed convection parameter  $\lambda$ , velocity slip parameter  $\alpha_1$  and volume fraction  $\phi$  with  $Pr = 6.2$ .

$\lambda$	$\alpha_1$	$\phi$	$\left(\frac{m+1}{2}\right)^{1/2} \frac{f''(0)}{(1-\phi)^{2.5}}$	$-\left(\frac{m+1}{2}\right)^{1/2} \theta'(0)$
-1.5	0.2	0.1	0.63293	2.03664
-1			0.66654	2.06641
0			0.73026	2.12071
0.5			0.76061	2.14567
1			0.79009	2.16938
1.5			0.25	0.81878
	0.75	0.76647	2.26216	
	1	0.2	0.45621	2.59342
		0.25	0.37729	2.66118
		0.3	0.40615	2.44402
			0.25	0.41788
		0.3	0.42834	2.22629

## Chapter 3

### Buongiorno model for slip flow past a flat plate with variable free stream velocity

#### 3.1 Introduction

In this chapter, boundary layer formation over a flat horizontal plate with stream wise pressure gradient is studied. Two-phase Buongiorno model is accounted to forecast the roles of Brownian diffusion and thermophoresis effects attributed to the presence of nanoparticles. Slip conditions and zero nanoparticle mass flux assumption are invoked and self-similarity solution is derived using MATLAB's bvp4c.

#### 3.2 Basic Equations and Similarity Transformations

Assume that nanofluid motion occurs over a flat horizontal plate at rest with a variable free stream velocity of power-law  $U(x) = ax^m$ , where  $a$  is constant and  $m$  is pressure gradient power law parameter (see Fig. 3.1). If  $(u, v)$  denote velocities along horizontal and vertical directions,  $T$  designates local temperature and  $\varphi$  stands for nanoparticle concentration, then conservation equations can be written in the following manner:

$$\frac{\partial u}{\partial x} + \frac{\partial v}{\partial y} = 0, \quad (3.1)$$

$$u \frac{\partial u}{\partial x} + v \frac{\partial u}{\partial y} = U \frac{dU}{dx} + \nu_{nf} \left( \frac{\partial^2 u}{\partial y^2} \right), \quad (3.2)$$

$$(\rho C_p)_{nf} \left( u \frac{\partial T}{\partial x} + v \frac{\partial T}{\partial y} \right) = k_{nf} \frac{\partial^2 T}{\partial y^2} + \rho_p C_p \left\{ C_B T \frac{\partial \varphi}{\partial y} \frac{\partial T}{\partial y} + C_T \frac{\varphi}{T} \left( \frac{\partial T}{\partial y} \right)^2 \right\}, \quad (3.3)$$

$$u \frac{\partial \varphi}{\partial x} + v \frac{\partial \varphi}{\partial y} = \frac{\partial}{\partial y} \left( C_B T \frac{\partial \varphi}{\partial y} + C_T \frac{\varphi}{T} \frac{\partial T}{\partial y} \right), \quad (3.4)$$

where  $C_B = D_B/T$  and  $C_T = D_T/\varphi$  are Brownian diffusion and thermophoresis diffusion coefficients respectively.  $\rho_{nf}, \nu_{nf}, k_{nf}, (\rho C_p)_{nf}$  denotes the effective density, kinematic

viscosity, thermal conductivity and volumetric heat capacity respectively. Since here we have ignored the variations in volume fraction  $\phi$  and hence set these nanofluids physical properties that are functions of  $\phi$  as kept constant or as same as of the base fluid.

Relevant boundary conditions are expressed below:

$$u = N(x)\mu_{nf} \frac{\partial u}{\partial y}, \quad v = 0, \quad T = T_w + D_1(x) \frac{\partial T}{\partial y}, \quad C_B T \frac{\partial \phi}{\partial y} + C_T \frac{\phi}{T} \frac{\partial T}{\partial y} = 0 \text{ at } y = 0, \quad (3.5)$$

$$u \rightarrow U, \quad T \rightarrow T_\infty, \quad \phi \rightarrow \phi_\infty \text{ as } y \rightarrow \infty.$$

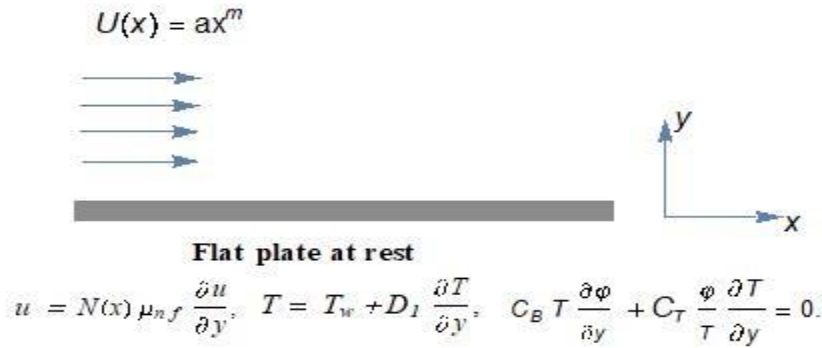


Fig. 3.1: Physical representation and coordinate system

Choosing the following similarity transformations [43]:

$$\eta = \left( \frac{(m+1)U(x)}{2\nu_{nf}x} \right)^{\frac{1}{2}} y, \quad \psi = \left( \frac{2\nu_{nf}xU(x)}{(m+1)} \right)^{\frac{1}{2}} f(\eta), \quad \theta(\eta) = \frac{T - T_\infty}{T_w - T_\infty}, \quad \chi(\eta) = \frac{\phi - \phi_\infty}{\phi_\infty}, \quad (3.6)$$

The governing equations (3.1) - (3.4) transform to the following ODEs:

$$f''' + ff'' + \frac{2m}{m+1}(1-f'^2) = 0, \quad (3.7)$$

$$\frac{1}{Pr_{nf}}\theta'' + f\theta' + Nt(1+\chi)(\theta')^2 + Nb\chi'\theta' = 0, \quad (3.8)$$

$$\chi'' + \frac{\Delta T}{T_\infty}\theta'\chi' + \frac{Nt}{Nb}\left\{\theta'\chi' + (1+\chi)\theta'' - (1+\chi)(\theta')^2\frac{\Delta T}{T_\infty}\right\} + Scf\chi' = 0, \quad (3.9)$$

where  $\Delta T = (T_w - T_\infty)$ ,  $Pr_{nf}$  defines the nanofluid Prandtl number,  $Nt$  and  $Nb$  are termed as Brownian motion and thermophoresis parameters and  $Sc$  defines the Schmidt number. The assumption used by Buongiorno that  $\Delta T \ll T_\infty$  allowing us to replace  $\Delta T\theta(\eta) + T_\infty$  with  $T_\infty$  while deriving Eqs. (3.7)-(3.9). The dimensionless parameters appearing in (3.7)-(3.9) are:

$$Pr_{nf} = \frac{(\rho C_p)_{nf} v_{nf}}{k_{nf}}, \quad (3.10)$$

$$Nt = \frac{C_T \varphi_\infty \Delta T \rho_p C_p}{T_\infty v_{nf} (\rho C_p)_{nf}}, \quad Nb = \frac{C_B T_\infty \varphi_\infty \rho_p C_p}{v_{nf} (\rho C_p)_{nf}}, \quad Sc = \frac{v_{nf}}{C_B T_\infty}.$$

Furthermore, the boundary conditions (3.5) assume the following forms:

$$f = 0, \quad \alpha_2(m+1)^{\frac{1}{2}}f'' = f', \quad 1 + \gamma_1(m+1)^{\frac{1}{2}}\theta' = \theta, \quad \chi' + \frac{Nt}{Nb}(1+\chi)\theta' = 0 \quad \text{at } \eta = 0, \quad (3.11)$$

$$f' \rightarrow 1, \quad \theta \rightarrow 0, \quad \chi \rightarrow 0 \quad \text{as } \eta \rightarrow \infty.$$

The expressions of  $\alpha_2$  and  $\gamma_1$  are similar to those of  $\alpha_1$  and  $\gamma$  where  $v_f$  is replaced with  $v_{nf}$ .

The shear force at the plate is calculated as follows:

$$\tau_w = \mu_{nf} \left( \frac{\partial u}{\partial y} \right)_{y=0} = \mu_{nf} U(x) f''(0) \left( \frac{(m+1)U(x)}{2v_{nf}x} \right)^{\frac{1}{2}}. \quad (3.12)$$

Eq. (3.12) can be utilized to determine normalized skin friction  $C_f$  defined below:

$$C_f = \frac{\tau_w}{\rho_{nf} U^2}. \quad (3.13)$$

which can be transformed to the following:

$$(Re_x)_{nf}^{1/2} C_f = \left(\frac{m+1}{2}\right)^{1/2} f''(0), \quad (3.14)$$

where  $(Re_x)_{nf} = Ux/\nu_{nf}$  expresses the local Reynolds number.

The local Nusselt number is defined as:

$$Nu_x = \frac{xq_w}{k_{nf}(T_w - T_\infty)}, \quad (3.15)$$

where  $q_w = -k_{nf}(\partial T/\partial y)_{y=0}$  represents heat flux at the surface. Heat transfer rate can be estimate by using local Nusselt number. By transformation (3.6), Eqs. (3.15) converts to the following:

$$(Re_x)^{-1/2} Nu_x = -\left(\frac{m+1}{2}\right)^{1/2} \theta'(0). \quad (3.16)$$

### 3.3 Numerical Results and Discussion

The set of coupled PDEs (3.1) - (3.4) along with boundary conditions (3.5) are transformed in to similar forms via generalized Blasius transformations (3.6). Similar to the Chapter 2, the self-similar system is evaluated numerically by MATLAB routine bvp4c. In this section, our entire focus will be to understand any contribution of diffusion coefficients on nanofluid heat transport phenomena.

Consequences of the change in Brownian diffusion effect on the concentration profile are illustrated graphically in Fig. 3.1. In light of Eq. (3.10), one can express  $Nb = \frac{1}{Sc} \left( \frac{\phi_\infty \rho_p c_p}{(\rho c_p)_{nf}} \right)$ . It implies that change in  $Nb$  can be linked with the corresponding change in  $Sc$ . Due to this reason, the values of Schmidt number  $Sc$  are adjusted for all selected values of  $Nb$  in Fig. 3.1. Brownian motion refers to the random motion of nanoparticles in that base fluid. As Brownian diffusion strengthens, the concentration boundary layer expands indicating that the presence of nanoparticles in larger extent of the fluid.

In order to figure out how the thermophoretic diffusion influences the nanofluid medium, we computed concentration profiles for various choices of  $Nt$  in Fig. 3.2. In thermophoretic diffusion, nanoparticles surrounding the hot surface are driven away from it (i.e. towards the region of lower temperature gradient). The expression of  $Nt$  clearly suggests that variation in  $Nt$  can be caused by the corresponding change in temperature difference  $\Delta T$ . As expected, the  $\chi$ -profile becomes broader/thicker for higher values of  $Nt$ .

It is worth-pointing here that contribution of  $Nb$  and  $Nt$  on temperature/heat transfer rate is not observed, which is also explained in detail by Myers *et al.* [33].

To visualize the contribution of pressure gradient parameter  $m$  on  $\chi$ , Fig. 3.3 is presented. A marked reduction in concentration penetration depth is witnessed for increasing  $m$ -values.

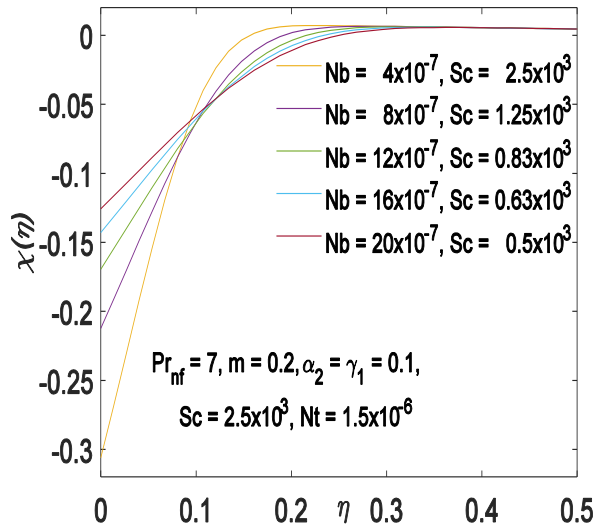


Fig. 3.1: Variation in concentration profile  $\chi(\eta)$  with  $\eta$  for different values of  $Nb$ .

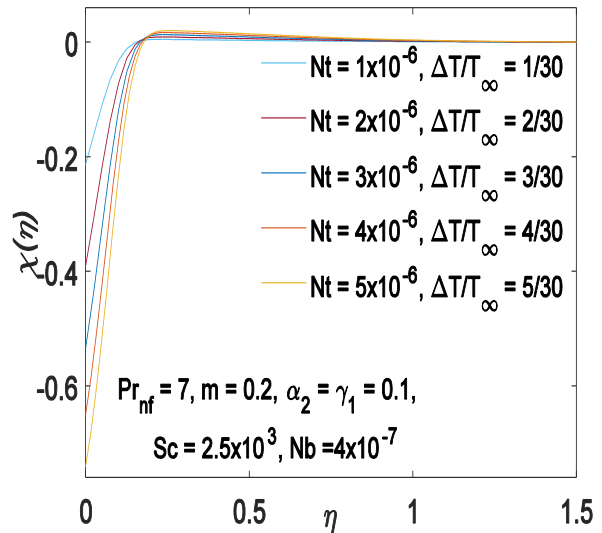


Fig. 3.2: Effects of different values of  $Nt$  on concentration profile  $\chi(\eta)$  with  $\eta$ .

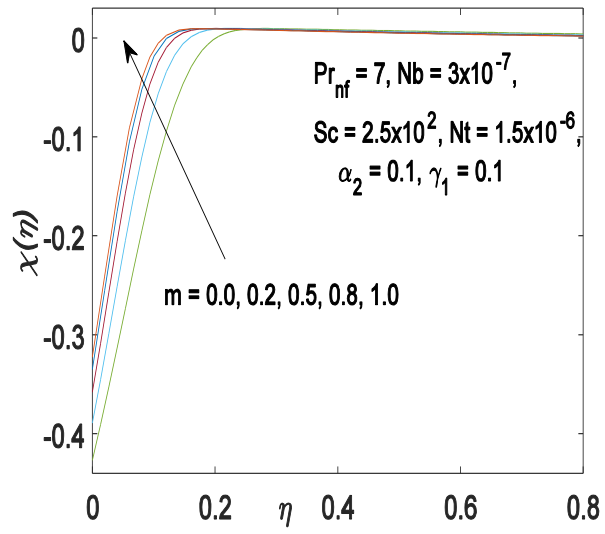


Fig. 3.3: Variation in concentration profile  $\chi(\eta)$  with  $\eta$  for different values of  $m$ .

## Chapter 4

### Conclusion and Future Works

In this thesis, first we have studied the buoyancy effects in Falkner-Skan flow of water based nanofluids under partial slip boundary conditions using Tiwari and Das model. The accompanying heat transfer process inspired by the buoyancy effect is also addressed under assisting and opposing flow scenarios. Here correct version of buoyancy force term arising for the Falkner-Skan problem is just derived. Secondly, we have studied two phase Buongiorno model to analyse slip flow past a flat plate with variable free stream velocity. Here the volume fraction of nanoparticle is kept constant while taken in to account the concentration of nanoparticles.

Observations drawn on the basis of numerical simulations are outlined as follows:

- A considerable growth in the thermal boundary layer thickness is found when nanoparticle volume fraction is considered; consequently, the wall slope of temperature profile  $\theta'(0)$  measuring the wall heat transfer rate decreases for increasing value of  $\phi$ .
- Naturally, buoyancy force term assists or opposes the fluid motion along the wedge surfaces for positive and negative values of  $\lambda$  respectively.
- Variations in computational results by changing parameter  $\lambda$  appear similar with and without addition of nanoparticles.
- In the existence of wall slip parameter, the momentum boundary layer is considerably suppressed compared with the corresponding no-slip case.
- The presence of thermal slip leads to the thinning of temperature profile which results in enhanced heat transfer from the surface.
- When there is an increase in mixed convection parameter  $\lambda$ , a noticeable increase in the values of wall shear is observed.
- Increasing the value of  $Pr$  results in the increase of the heat transfer rate.
- For Cu – water and  $Al_2O_3$  – water, the skin friction coefficient and the Nusselt number have highest and lowest values respectively.



- The Brownian parameter  $Nb$  and thermophoresis parameter  $Nt$  have no effect on temperature profiles while they do have effects on the concentration profiles. Higher and lower concentration is associated with an increase in Brownian motion and thermophoresis motion respectively.
- The concentration profile( $\chi$ ) has a direct relation with the pressure gradient power parameter  $m$ , measuring favourable pressure gradient.

The Tiwari and Das model has revealed the significant results to focus on the pressure gradient effects, slip effects and volume fraction of nanoparticles on the flow of nanofluids over static wedge whereas the Buongiorno model indicated the Brownian and thermophoresis effects on the concentrations profile. Future research could look in to the use of temperature dependent thermal conductivity, viscous dissipation, convective boundary conditions and MHD fluid flow and heat transfer of nanofluids for falkner-Skan flow over static/moving wedge.

## Bibliography

1. V. M. Falkner and S. W. Skan, Some approximate solutions of the boundary layer equations, *Philos. Maga.* 12 (1931) 865-896.
2. D.R. Hartree, On the equation occurring in Falkner and Skan's approximate treatment of the equations of the boundary layer, *Proc. Camb. Philos. Soc.* 33 (1937) 223-239.
3. H. C. Brinkman, The viscosity of concentrated suspensions and solutions, *J. Chem. Phys.* 20 (1952) doi: 10.1063/1.1700493.
4. H. F. Oztop and E. Abu-Nada, Numerical study of natural convection in partially heated rectangular enclosures filled with nanofluids, *Int. J. Heat Fluid Flow*, 29 (2008) 1326-1336.
5. J. C. Maxwell, *A treatise on electricity and magnetism*, 2nd Ed. Cambridge: Oxford University Press; 1904. pp. 435-41.
6. J. Buongiorno, Convective Transport in Nanofluids, *J. Heat Transf.* 128 (2006) 240-250
7. K. Stewartson, Further solutions of the Falkner–Skan equation, *Proc. Camb. Philos. Soc.* 50 (1954) 454–465.
8. H. T. Yang and L. C. Chien, Analytic solutions of the Falkner-Skan equation when  $\beta = -1$  and  $\gamma = 0$ , *SIAM J. Appl. Math.* 29 (1975) 558-569.
9. C. M. Brauner, Cl. Laine and B. Nicolaenko, Further solutions of the Falkner–Skan equation for  $\beta = -1$  and  $\gamma = 0$ , *Mathematika* 29 (1982) 231-248.
10. K. R. Rajagopal, A. S. Gupta and T. Y. Na, A note on the Falkner-Skan flows of a non-Newtonian fluid, *Int. J. Non-Linear Mech.* 18 (1983) 313-320.
11. T. Watanabe, Thermal boundary layers over a wedge with uniform suction or injection in forced flow, *Acta Mech.* 83 (1990) 119-126.
12. K. A. Yih, Uniform suction/blowing effect on forced convection about a wedge: uniform heat flux, *Acta Mech.* 128 (1998) 173–181.
13. A. Asaithambi, A finite-difference method for the Falkner-Skan equation, *Appl. Math. & Comput.* 92 (1998) 135-141.
14. D. O. Olagunju, The Falkner–Skan flow of a viscoelastic fluid, *Int. J. Non-Linear Mech.* 41 (2006) 825-829.

15. N. A. Yacob, A. Ishak and I. Pop, Falkner-Skan problem for a static or moving wedge in nanofluids, *Int. J. Therm. Sci.* 50 (2011) 133-139.
16. T. Fang, S. Yao, J. Zhang, Y. Zhong and H. Tao, Momentum and heat transfer of the Falkner–Skan flow with algebraic decay: an analytic solution, *Commun. Nonlinear Sci. Numer. Simul.* 17 (2012) 2476–2488.
17. T. Hayat, M. Farooq and Z. Iqbal, Mixed Convection Falkner–Skan Flow of a Maxwell Fluid, *J. Heat Transf.* 134 (2012) Article ID: 114504.
18. M. Turkyilmazoglu, Slip flow and heat transfer over a specific wedge: an exactly solvable Falkner–Skan equation, *J. Eng. Math.* 92 (2015) 73–81.
19. J. H. Merkin, Mixed Convection in a Falkner-Skan system, *J. Eng. Math.* 100 (2016) 167–185.
20. K. Das, N. Acharya and P. K. Kundu, Influence of variable fluid properties on nanofluid flow over a wedge with surface slip, *Arab. J. Sci. Eng.* 43 (2018) 2119–2131.
21. S. Dinarvand, A novel hybridity model for TiO<sub>2</sub>- CuO/water hybrid nanofluid flow over a static/moving wedge or corner, *Scientific Reports*, 9 (2019) Article ID: 16290.
22. I. S. Awaludin, A. Ishak, I. Pop, On the stability of MHD boundary layer flow over a stretching/shrinking wedge, *Scientific Reports* 8 (2018), Article ID: 13622.
23. C. Y. Wang, Heat transfer from a concentrated tip source in Falkner-Skan flow, *J. Heat Transf.* 143 (2021) Article ID: 094502.
24. J. A. Eastman, S. U. S. Choi, S. Li, W. Yu and L. J. Thompson, Anomalous increased effective thermal conductivities of ethylene glycol-based nanofluids containing copper nanoparticles, *Appl. Phys. Lett.* 78 (2001) 718-720.
25. M. M. Tawfik, Experimental studies of nanofluid thermal conductivity enhancement and applications, *Renewable and Sustainable Energy Reviews*, 75 (2017) 1239-1253.
26. G. Humnic and A. Humnic, Entropy generation of nanofluid and hybrid nanofluid flow in thermal systems: A review, *J. Molec. Liq.* 302 (2020) Article ID: 112533.
27. I. Wole-Osho, E. C. Okonkwo, S. Abbasoglu and D. Kavaz, Nanofluids in Solar Thermal Collectors: Review and Limitations, *Int. J. Thermophysics* 41 (2020) 1-74.
28. D. A. Nield and A. V. Kuznetsov, The Cheng–Minkowycz problem for the double-diffusive natural convective boundary layer flow in a porous medium saturated by a nanofluid, *Int. J. Heat & Mass Transf.* 54 (2011) 374-378.

29. A. V. Kuznetsov and D. A. Nield, Double-diffusive natural convective boundary-layer flow of a nanofluid past a vertical plate, *Int. J. Therm. Sci.* 50 (2011) 712-717.
30. A. V. Kuznetsov and D. A. Nield , Natural convective boundary-layer flow of a nanofluid past a vertical plate: A revised model, *Int. J. Therm. Sci.* 77 (2014) 126-129.
31. D. A. Nield and A. V. Kuznetsov, Forced convection in a parallel-plate channel occupied by a nanofluid or a porous medium saturated by a nanofluid, *Int. J. Heat & Mass Transf.* 70 (2014) 430-433.
32. D. A. Nield and A. V. Kuznetsov, The onset of convection in a horizontal nanofluid layer of finite depth: A revised model, *Int. J. Heat & Mass Transf.* 77 (2014) 915-918.
33. T. G. Myers, H. Ribera and V. Cregan, Does mathematics contribute to the nanofluid debate?, *Int. J. Heat & Mass Transf.* 111 (2017) 279-288.
34. S. Dinarvand, R. Hosseini, M. Abdulhasansari and I. Pop, Buongiorno's model for double-diffusive mixed convective stagnation-point flow of a nanofluid considering diffusiophoresis effect of binary base fluid, *Adv. Powder Technol.* 26 (2015) 1423-1434.
35. M. Mustafa, MHD nanofluid flow over a rotating disk with partial slip effects: Buongiorno model, *Int. J. Heat & Mass Transfer* 108 (2017) 1910-1916.
36. M. A. Sheremet, C. Revnic and I. Pop, Natural convective heat transfer through two entrapped triangular cavities filled with a nanofluid: Buongiorno's mathematical model, *Int. J. Mech. Sci.* 133 (2017) 484-494.
37. M. Turkyilmazoglu, Buongiorno model in a nanofluid filled asymmetric channel fulfilling zero net particle flux, *Int. J. Heat & Mass Transfer* 126 (2018) 974–979.
38. R. J. Tiwari and M. K. Das, Heat transfer augmentation in two-sided lid-driven differentially heated square cavity utilizing nanofluids, *Int. J. Heat & Mass Transf.* 50 (2007) 2002-2018.
39. H. F. Oztop and E. Abu-Nada, Numerical study of natural convection in partially heated rectangular enclosures filled with nanofluids, *Int. J. Heat & Fluid Flow* 29 (2008) 1326-1336.
40. M. A. Sheremet, S. Dinarvand and I. Pop, Effect of thermal stratification on free convection in a square porous cavity filled with a nanofluid using Tiwari and Das' nanofluid model, *Physica E* 69 (2015) 323-341.

41. M. Turkyilmazoglu, Fully developed slip flow in a concentric annuli via single and dual phase nanofluids models, *Comput. Meth. & Prog. Biomed.* 179 (2019), Article ID: 104997.
42. A. A. Siddiqui and M. Turkyilmazoglu, Natural convection in the ferrofluid enclosed in a porous and permeable cavity, *Int. Commun. Heat & Mass Transf.* 113 (2020), Article ID: 104499.
43. F. M. White, *Viscous Fluid Flow* (3rd ed.), McGraw-Hill, New York, 2006.
44. L. Rosenhead, *Laminar boundary layer*, Oxford University Press, Oxford, 1963.